PHYSICAL REVIEW LETTERS

Excitonic Effects and Optical Properties of Passivated CdSe Clusters

Marie Lopez del Puerto,[1] Murilo L. Tiago,[2] and James R. Chelikowsky[1,2,3]

[1]*Department of Physics, University of Minnesota, Minneapolis, Minnesota 55455, USA*
[2]*Center for Computational Materials, Institute for Computational Engineering and Sciences, University of Texas,
Austin, Texas 78712, USA*
[3]*Departments of Physics and Chemical Engineering, University of Texas, Austin, Texas 78712, USA*

We calculate the optical properties of a series of passivated nonstoichiometric CdSe clusters using two first-principles approaches: time-dependent density functional theory within the local-density approximation, and by solving the Bethe-Salpeter equation for optical excitations with the *GW* approximation for the self-energy. We analyze the character of optical excitations leading to the first low-energy peak in the absorption cross section of these clusters. Within time-dependent density functional theory, we find that the lowest-energy excitation is mostly a single-level to single-level transition. In contrast, many-body methods predict a strong mixture of several different transitions, which is a signature of excitonic effects. The majority of the clusters have a series of dark transitions before the first bright transition. This may explain the long radiative lifetimes observed experimentally.

Experimental advances in the synthesis of semiconductor clusters have stimulated considerable theoretical effort to understand the optical and electronic properties of these systems. Semiconductor clusters often exhibit strong size-dependent effects, which are not yet fully understood. As an intermediate system between single atoms and bulk materials, semiconductor clusters are also of intrinsic theoretical interest. Clusters of II-VI elements, such as CdSe, have attracted considerable attention in recent years owing to their potential technological applications in various devices such as solar cells, lasers, and biological imaging tools, among others [1]. Great effort has gone into fabricating and characterizing size-controlled samples. This is particularly challenging because clusters of different sizes have similar stoichiometry and are synthetized by similar reactions in which the temperature, the solvent, and the ratio and concentration of precursors have to be carefully controlled [2]. Theoretical calculations are difficult because of the inherent complexity of accurate theories, as we can infer from the limited number of theoretical articles in the literature [3–6].

The use of pseudopotentials and density functional theory (DFT) have been very successful in determining the ground-state properties of both bare [3] and passivated [5] CdSe clusters. However, DFT is a ground-state theory, and it has serious shortcomings in providing a quantitative description of optical and electronic excitations [7,8]. Understanding spectroscopic experiments requires the computation of excited state properties, which present a greater challenge than ground-state calculations. The problem is addressed by both time-dependent density functional theory (TDDFT) and *GW*-Bethe-Salpeter (*GW*-BSE) methods. TDDFT is simpler to implement, but a good general approximation for the exchange-correlation functional is still lacking [7]. The local-density approximation within TDDFT (TDLDA) has been found to give accurate results

for some finite systems such as sodium clusters [9]. In others, it gives at best a qualitative picture [6,7,10]. On the other hand, *GW*-BSE has been shown to be very accurate in bulk materials [7,8], albeit more computationally demanding. Until recently, first-principles *GW*-BSE calculations have been done only for very small clusters, containing no more than 35 atoms [6–8,11].

In this Letter we present a detailed comparison of TDLDA and *GW*-BSE calculations of the optical properties of passivated CdSe clusters. By examining the character of the transition leading to the first peak in the absorption spectra, we investigate the importance of many-body effects, fully accounted for in *GW*-BSE but absent in TDLDA. Calculations of energy band gaps and absorption spectra of bare CdSe clusters have been done using TDDFT within the local-density approximation (TDLDA) [3]. Energy band gaps of passivated CdSe clusters have also been calculated within the TDDFT framework [5]. *GW*-BSE has been used for calculations of optical properties of molecular systems, silicon clusters, and in crystals [7,8,11,12], but not III-V or II-VI clusters yet. Experimental data on CdSe clusters is readily available [2], which makes these systems ideal for a comparative analysis.

We studied a series of five clusters: Cd_4Se_6, Cd_8Se_{13}, $Cd_{10}Se_{16}$, $Cd_{17}Se_{28}$, and $Cd_{32}Se_{50}$. While larger CdSe clusters are found to be spherical [13], these smaller clusters are of pyramidal shape [2] (see Fig. 1). Two of the clusters studied have zinc blende structures (Cd_4Se_6 and $Cd_{10}Se_{16}$), while the rest are of the wurtzite type. All clusters were passivated by fictitious hydrogen atoms of charge $1.5e$ (attached to surface Cd atoms) and $0.5e$ (attached to surface Se atoms) [14], in order to simulate the effect of surfactants on the surface of the real clusters [2].

The initial geometry of the clusters was constructed based on the x-ray data [2] and then relaxed [15,16].
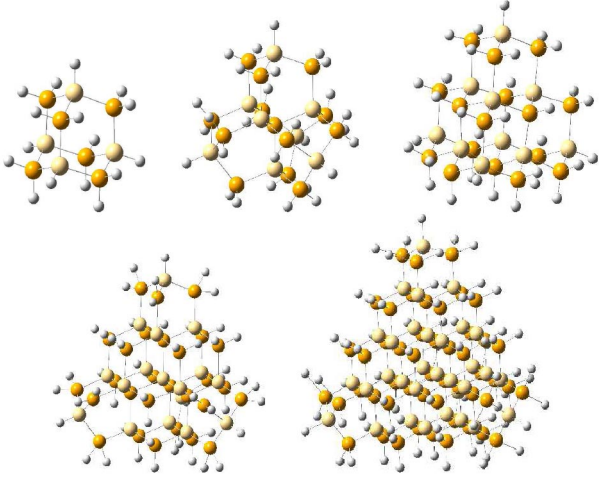
FIG. 1 (color online).   Geometry of the clusters studied: Cd_4Se_6, Cd_8Se_{13}, $Cd_{10}Se_{16}$, $Cd_{17}Se_{28}$, and $Cd_{32}Se_{50}$. Cd atoms are dark yellow, Se atoms are light yellow, and fictitious H atoms are small gray.

Tetrahedral symmetry was conserved during the relaxation. The CdSe bonds in the final structures are comparable to the experimental measurements [2], but about 5% shorter than the CdSe bond in bulk cadmium selenide. Calculations were done using norm-conserving pseudopotentials [17] constructed within the local-density approximation of density functional theory. Pseudopotentials for cadmium and selenium have scalar relativistic effects included and the interaction between the Cd $4d$ orbital and valence orbitals is accounted for by a nonlinear core correction in the pseudopotential [18]. Spin-orbit and semicore effects beyond the nonlinear core correction are ignored. In order to estimate how important these effects are, we computed the band gap of bulk CdSe in the wurtzite structure. The gap obtained within the GW approximation is 1.8 eV, which compares well with the spin-orbit averaged gap obtained in experiment: 1.97 eV [19]. The mea-

sured spin-orbit splitting, Δ, at the valence band maximum at the Γ point is $\Delta = 0.43$ eV [19]. Including spin-orbit splitting would change the calculated energy gap by $E_{\text{gap}} = \frac{\Delta}{3} \sim 0.15$ eV. The Kohn-Sham equations are solved on a real space grid using a higher-order finite difference method [20]. All calculations were done within a spherical boundary of radius at least 6 a.u. from the outermost passivating atoms. A grid spacing of 0.3 a.u. was used for LDA calculations, while a grid spacing of 0.6 a.u. was used for the calculation of optical properties as described below.

In TDLDA [21,22], the optical response is evaluated as a first-order perturbation in the electron density due to an external potential. The excitation energies Ω_n are obtained from a solution of the eigenvalue equation [21,22]:

$$\mathbf{Q}\mathbf{F}_n = \Omega_n^2 \mathbf{F}_n. \tag{1}$$

The matrix elements for $\mathbf{Q}$ are given by

$$Q_{ij\sigma,kl\tau} = \delta_{i,k}\delta_{j,l}\delta_{\sigma,\tau}\hbar^2\omega_{kl\tau}^2 + 2\hbar\sqrt{\lambda_{ij\sigma}\omega_{ij\sigma}}K_{ij\sigma}^{kl\tau}\sqrt{\lambda_{kl\tau}\omega_{kl\tau}}, \tag{2}$$

where $\lambda_{kl\tau} = n_{l\tau} - n_{k\tau}$ is the difference between the occupation numbers, and $\hbar\omega_{lk\tau} = \epsilon_{k\tau} - \epsilon_{l\tau}$ is the difference between the eigenvalues of the single-particle states. K is the coupling matrix which describes the linear response of the system [21].

Electron-phonon coupling and temperature dependence effects are included *a posteriori* by broadening the absorption spectra with a normalized Gaussian function with fixed dispersion of 0.1 eV.

In the GW-BSE method, the many-body expression for the polarizability Π is related to the electron-hole correlation function L by

$$\Pi(1, 2) = -iL(1, 2; 1^+, 2^+), \tag{3}$$

where L satisfies the Bethe-Salpeter equation [7,8]:

$$L(1, 2; 3, 4) = G(1, 4)G(2, 3) + \int d(5678)G(1, 5)G(6, 3)K(5, 7; 6, 8)L(8, 2; 7, 4). \tag{4}$$

Solving the above equation, we obtain optical excitations of the electronic system. G is the electron Green's function, and the kernel operator K describes interactions between the excited electron and the hole left behind in the electron sea. The electron self-energy is calculated within the GW approximation [23]. As in TDLDA, the absorption spectra is broadened by normalized Gaussian functions with fixed dispersion. In both TDLDA and GW-BSE, the optical gap is defined as the energy of the first transition with measurable oscillatory strength (the first allowed transition) [22].

Figure 2 shows optical gaps as a function of CdSe cluster size. For all but the smallest cluster, our calculations [5] show a trend very similar to that found in experiment. The dependence of the gap on cluster size is very strong. It is interesting to note that while TDLDA calculations under-

estimate the gap by $\sim$0.5 to $\sim$1.5 eV, GW-BSE overestimates the gap by less than 0.6 eV. The discrepancy between experimental data and TDLDA calculations increases as the size of the cluster increases, but the opposite is observed for GW-BSE calculations. Based on the analysis made for bulk CdSe, we expect that neglected spin-orbit and semicore effects at the pseudopotential level are responsible for a residual discrepancy between theory and experiment of a few tenths of an electron volt.

There is a large discrepancy between the theoretical calculations and the experimental measurements for the optical gap of the smallest cluster, Cd_4Se_6. For the larger clusters, all TDLDA results are below experiment, while BSE results are above. This is not the case for Cd_4Se_6, as both TDLDA and BSE predict larger optical gaps than measured experimentally. Given the reduced number of
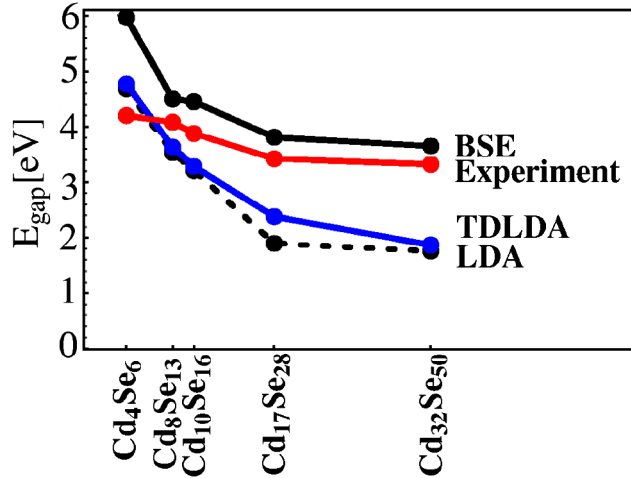
FIG. 2 (color online). Experimental and calculated optical gaps. The LDA gap is simply the difference between Kohn-Sham eigenvalues.

atoms in this cluster, it is not clear whether the organic ligands on the surface or some other mechanism might be responsible for this discrepancy.

Calculated absorption cross sections (normalized by the total number of cadmium and selenium atoms in each cluster) are shown in Fig. 3. Both TDLDA and BSE have a well-defined first peak at low energy, with a second peak separated from the first by ~ 1 eV. We have analyzed the character of the excitation leading to the first peak observed in the absorption cross section. As shown in Table I, the first TDLDA excitation in all clusters is mostly a result of single-level to single-level transitions. For the three smallest clusters, the dominant transition is from the
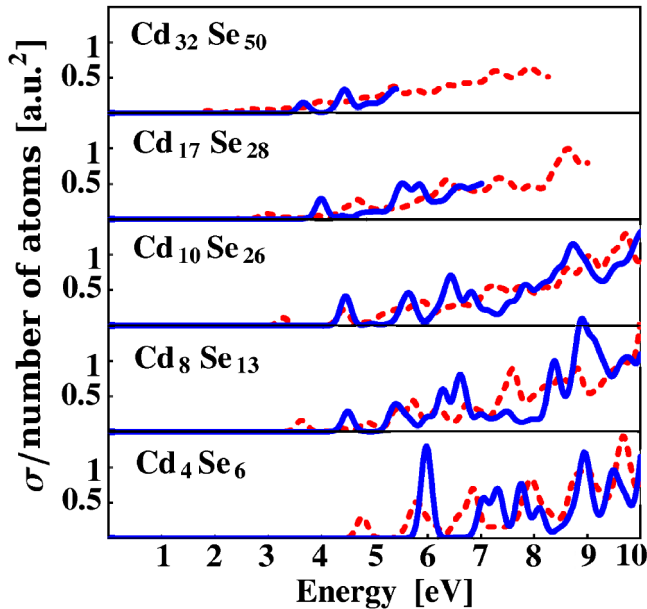
highest occupied molecular orbital (HOMO), which is triple-degenerate for most clusters, without spin-orbit splitting, to the lowest unoccupied molecular orbital (LUMO), which is nondegenerate in all cases. This is not so for the two largest clusters as they have a series of dark transitions (transitions with negligible oscillatory strength) before the first bright (allowed) transition. The first optically allowed transition for $Cd_{17}Se_{28}$ involves transitions from the third level below the HOMO to the LUMO. For $Cd_{32}Se_{50}$ the first allowed transition is from the first level below the HOMO to the LUMO.

Experimentally, bulk CdSe in the wurtzite and zinc blende structures is a direct gap semiconductor [24]. Our own LDA calculations agree with these experimental results. Clusters, however, do not always behave in the same way. This can be attributed to confinement effects and the geometry of each cluster [25,26]. Cd_4Se_6, Cd_8Se_{13}, and $Cd_{10}Se_{16}$ have dipole allowed transitions between the triple-degenerate HOMO and the nondegenerate LUMO. But the HOMO of $Cd_{17}Se_{28}$ is nondegenerate because of a change in the ordering of the energy levels (the HOMO-1 is triple-degenerate), and the HOMO-LUMO transition becomes dipole forbidden as a result of selection rules. $Cd_{32}Se_{50}$ has a dipole allowed HOMO-LUMO transition, but the oscillator strength is small because of little overlap between HOMO and LUMO wave functions.

The character of the *GW*-BSE excitation leading to the first peak in the absorption spectra is very different from the one predicted by TDLDA. For the smallest cluster the excitation is still dominated by a single-level to single-level (HOMO $\rightarrow$ LUMO) transition. For the rest of the clusters, however, the excitation is the result of a strong mixture of different transitions. There are two sources of mixing in *GW*-BSE: at the *GW* level, mixing occurs because of the fact that LDA wave functions are not identical to quasiparticle wave functions [6,8,23]; at the BSE level, the electron-hole kernel is stronger and more nonlocal than the TDLDA kernel. We find that the mixing in TDLDA is 1 order of magnitude smaller than the mixing in *GW*-BSE.

FIG. 3 (color online). Absorption cross section calculated within TDLDA (dashed curve) and *GW*-BSE (solid curve).

TABLE I. Energy of the first allowed transition, E; presence of dark transitions (those with negligible oscillatory strength) before the first allowed transition; and percentage of the lowest-energy peak in the absorption cross section that is due to the single-level to single-level transition indicated in the text. No entry in the percentage column indicates that the transition is strongly mixed, i.e, the largest component contributes less than 25%.

Cluster	TDLDA			*GW*-BSE		
	E [eV]	Dark	%	E [eV]	Dark	%
Cd_4Se_6	4.77	no	96	5.97	yes	91
Cd_8Se_{13}	3.53	no	94	4.50	no	
$Cd_{10}Se_{16}$	3.21	no	96	4.45	yes	
$Cd_{17}Se_{28}$	2.38	yes	98	3.81	yes	
$Cd_{32}Se_{50}$	1.87	yes	98	3.65	yes	

This is a result of stronger coupling matrix elements at the GW-BSE level compared to TDLDA. We quantify the mixing as

$$M = \frac{\Sigma_i \Sigma_{j \neq i} |H_{ij}|^2}{\Sigma_i |H_{ii}|^2}, \qquad (5)$$

where H is the effective Hamiltonian matrix in either TDLDA or GW-BSE methods. $M = 0$ corresponds to a situation where there is no mixing between different single electron transitions. We find that the mixing M within GW-BSE is of the order of 10^{-2} while within TDLDA it is of the order of 10^{-3}. In both cases the mixing is nonzero but still much smaller than 1. As a result of the stronger mixing in GW-BSE, the excitation cannot be associated with a single electron-hole transition. A similar behavior has been observed in small silicon clusters and in bulk semiconductors [7,8], and it is a signature of excitonic effects.

The effects of mixing also explain the observed divergence in the experimental and TDLDA curves in Fig. 2. Since the energy levels in the smaller clusters are more separated, the mixing effect is not as large and TDLDA calculations are more accurate than for larger clusters where the energy levels are closer together and more mixing can occur.

In the GW-BSE calculations we find that there are dark transitions for all clusters but Cd_8Se_{13}. Van Driel *et al.* [4] have recently shown that measured rates of emission are completely determined by radiative decay and that the occupation of dark excitonic states considerably attenuates spontaneous emission. The presence of dark transitions in our GW-BSE calculations then may explain in part the long radiative lifetimes ($\sim$1–10 μs) observed experimentally.

In conclusion, we have calculated the optical properties of a series of small CdSe clusters using two different approaches: TDLDA and GW-BSE. We find that the two methods lead to a very different character for the lowest-energy excitation. In TDLDA, the excitation is dominated by a single-level to single-level transition. In GW-BSE, however, the excitation is the result of strong mixing between different transitions. We interpret this as due to exciton effects. Our calculations also show that most clusters have a series of dark transitions before the first bright transition, which attenuates spontaneous emission and may explain the long radiative lifetimes of these clusters.

[1] W. U. Huynh *et al.*, Science **295**, 2425 (2002); X. Michalet *et al.*, Science **307**, 538 (2005); S. Coe *et al.*, Nature (London) **420**, 800 (2002); W. C. W. Chan and S. M. Nie, Science **281**, 2016 (1998); V. I. Klimov *et al.*, Science **290**, 314 (2000).
[2] V. N. Soloviev *et al.*, Phys. Status Solidi B **224**, 285 (2001); V. N. Soloviev *et al.*, J. Am. Chem. Soc. **122**, 2673 (2000); V. N. Soloviev *et al.*, J. Am. Chem. Soc. **123**, 2354 (2001).
[3] M. C. Troparevsky *et al.*, Phys. Rev. B **65**, 033311 (2001).
[4] A. F. van Driel *et al.*, Phys. Rev. Lett. **95**, 236804 (2005).
[5] K. Eichkorn and R. Ahlrichs, Chem. Phys. Lett. **288**, 235 (1998).
[6] M. L. Tiago and J. R. Chelikowsky, Phys. Rev. B **73**, 205334 (2006).
[7] G. Onida *et al.*, Rev. Mod. Phys. **74**, 601 (2002).
[8] M. Rohlfing and S. G. Louie, Phys. Rev. B **62**, 4927 (2000); G. Strinati, Riv. Nuovo Cimento **11**, 1 (1988).
[9] I. Vasiliev, S. Öğüt, and J. R. Chelikowsky, Phys. Rev. Lett. **82**, 1919 (1999).
[10] M. Lopez del Puerto *et al.*, Phys. Rev. A **72**, 052504 (2005).
[11] L. X. Benedict, Phys. Rev. B **68**, 085310 (2003).
[12] S. Behrens *et al.*, Angew. Chem., Int. Ed. Engl. **35**, 2215 (1996).
[13] J. E. B. Katari *et al.*, J. Phys. Chem. **98**, 4109 (1994); C. B. Murray *et al.*, J. Am. Chem. Soc. **115**, 8706 (1993).
[14] X. Huang *et al.*, Phys. Rev. B **71**, 165328 (2005).
[15] R. H. Byrd *et al.*, SIAM J. Sci. Stat. Comput. **16**, 1190 (1995).
[16] C. Zhu *et al.*, ACM Trans. Math. Softw. **23**, 550 (1997).
[17] N. Troullier and J. Martins, Phys. Rev. B **43**, 1993 (1991).
[18] S. G. Louie *et al.*, Phys. Rev. B **26**, 1738 (1982).
[19] Quoted by O. Zakharov *et al.*, Phys. Rev. B **50**, 10780 (1994).
[20] J. R. Chelikowsky *et al.*, Phys. Rev. Lett. **72**, 1240 (1994).
[21] M. E. Casida, in *Recent Advances in Density-Functional Methods*, edited by D. P. Chong (World Scientific, Singapore, 1995), Pt. I, p. 155; M. E. Casida, in *Recent Developments and Applications of Modern Density Functional Theory*, edited by J. M. Seminario (Elsevier Science, Amsterdam, 1996), p. 391.
[22] I. Vasiliev *et al.*, Phys. Rev. B **65**, 115416 (2002).
[23] M. S. Hybertsen and S. G. Louie, Phys. Rev. B **34**, 5390 (1986); W. G. Aulbur *et al.*, in *Solid State Physics*, edited by F. Seitz, D. Turbull, and H. Ehrenreich (Academic, New York, 2000), Vol. 54, p. 1.
[24] A. L. Edwards and H. G. Drickamer, Phys. Rev. **122**, 1149 (1961).
[25] S. H. Tolbert *et al.*, Phys. Rev. Lett. **73**, 3266 (1994).
[26] M. V. Rama Krishna and R. A. Friesner, J. Chem. Phys. **95**, 8309 (1991).